Evolutionary Conservation of Enzymatic Catalysis: Quantitative Comparison of the Effects of Mutation of Aligned Residues in *Saccharomyces cerevisiae* and *Escherichia coli* Inorganic Pyrophosphatases on Enzymatic Activity[†]

Pekka Pohjanjoki,[‡,§] Reijo Lahti,*[,‡] Adrian Goldman,[‡,||] and Barry S. Cooperman*[,§]

Department of Biochemistry, University of Turku, FIN-20014 Turku, Finland, Department of Chemistry, University of Pennsylvania, Philadelphia, Pennsylvania 19104, and Centre for Biotechnology, University of Turku and Åbo Akademi University, FIN-20521 Turku, Finland

Received July 21, 1997; Revised Manuscript Received October 16, 1997

ABSTRACT: Soluble inorganic pyrophosphatase (PPase) is one of the better understood phosphoryl-transfer enzymes and is distinctive in having four divalent metal ions at the active site. Here we determine pH profiles for wild-type *Saccharomyces cerevisiae* PPase (Y-PPase) and for 14 of its active site variants and consider the effects of active site mutation on the pH-independent parameters and acid dissociation constants that characterize these profiles against the framework of the proposed structure of the activated complex. The results obtained (a) support the current mechanistic model in which a hydroxide ion, stabilized by binding to two metal ions at the active site and by an extended system of hydrogen bonds within the active site, is the nucleophile that attacks enzyme-bound inorganic pyrophosphate and (b) provide evidence that the acid group that is necessary for maximal activity is a water molecule coordinated to a third metal ion, as shown by the general rise in the pK_a of this group that is a consequence of almost all of the mutations. We further compare the present results to those previously observed for the corresponding mutations in *Escherichia coli* PPase [E-PPase; Salminen *et al.* (1995) *Biochemistry 34*, 782−791]. Such comparison provides a measure of the extent to which different portions of the active site are conserved. We find that some corresponding mutations have different effects on catalytic function, demonstrating that even in the context of very similar active sites, interactions of the mutated site with less well conserved portions of the enzyme, in this case outside the active site, can lead to different outcomes. On the other hand, one region of the active site is highly conserved, suggesting that it may represent a common feature of phosphoryl-transfer enzymes or a vestige of a primitive ur-PPase active site.

Soluble inorganic pyrophosphatase (EC 3.6.1.1; PPase[1]), which hydrolyzes inorganic pyrophoshate (PP_i) to inorganic phosphate (P_i), is an essential enzyme (*1*−*3*), providing a thermodynamic pull for many biosynthetic reactions (*4*). With detailed structural and functional information now available [as summarized recently (*5*)] PPase is one of the better understood phosphoryl-transfer enzymes. A precise mechanism has been proposed to account for its catalytic efficiency, a factor of 10^{10} compared with the rate of PP_i hydrolysis in solution (*5*).

The best-studied soluble PPases are those from the yeast *Saccharomyces cerevisiae* (Y-PPase) (*6*−*10*) and from *Escherichia coli* (E-PPase) (*11*−*13*). Both of these enzymes require divalent metal ions for catalysis, with Mg^{2+} conferring the highest activity (*14*). Mg^{2+} has a dual role, both activating the enzyme and, as a magnesium pyrophosphate complex, forming part of the substrate. Y-PPase is active with either three or four magnesium ions per active site (*8, 15*). The minimal kinetic scheme for Y-PPase catalysis at neutral pH is shown in Scheme 1.

Scheme 1: Minimal Kinetic Scheme of Y-PPase Catalysis with Four Mg^{2+} Ions

$$EMg_2 + Mg_2PP_i \rightleftarrows EMg_2(Mg_2PP_i) \overset{H_2O}{\rightleftharpoons} EMg_2(MgP_i)_2 \rightleftarrows EMg_2(MgP_i) \rightleftarrows EMg_2 + MgP_i \quad (+MgP_i)$$

The active site of Y-PPase contains 14 to 15 polar residues that structurally align very well with the corresponding conserved residues in E-PPase (*5, 16*), out of a total of 17 polar residues originally implicated by Terzyan *et al.* (*17*) as being potentially important for catalytic activity. Recently, we described the expression and initial characterization of conservative variants at each of the 17 putative active site residues of Y-PPase (*18*) including measurements of thermostability, oligomeric structure, and specific activity at pH 7.2. In the present work we determine pH profiles for WT-Y-PPase and for 14 of these Y-PPase variants. We then consider the effects of active site mutation on the pH-independent parameters and acid dissociation constants that

[†] This work was supported by NIH Grant DK13212 and Grants 1444, 35736, 4310, and 28866 from the Finnish Academy of Science.

* Address correspondence to B.S.C. (Tel 215-898-6330; fax 215-898-2037; e-mail cooprman@pobox.upenn.edu) and R.L. (Tel 358-02-3336845; fax 358-02-3336860; e-mail reila@utu.fi).

[‡] University of Turku.

[§] University of Pennsylvania.

[||] University of Turku and Åbo Akademi University.

[1] Abbreviations: PPase, inorganic pyrophosphatase; E-PPase, *Escherichia coli* PPase; Y-PPase, yeast (*Saccharomyces cerevisiae*) PPase; WT, wild type; PP_i, pyrophosphate; P_i, phosphate.

S0006-2960(97)01771-6 CCC: $15.00
Published on Web 01/30/1998

Table 1: pH-Dependent Values of Equilibrium Constants Involving PP_i and Mg^{2+}

pH	K_A[a] (mM)	K_{A2}[a] (mM)
6.5	0.29	6.3
7.2	0.086	2.8
8.0	0.017	2.1
8.5	0.006	2.0
9.3	0.002	2.0
10.0	0.0015	2.0

[a] $K_A = [Mg][PP_i]_f/[MgPP_i]_t$; $K_{A2} = [Mg][MgPP_i]_f/[Mg_2PP_i]_t$. Values are derived from ref *20*.

characterize these profiles against the framework of the proposed structure of the activated complex as derived from the X-ray crystal structure of a Y-PPase product complex (*5*). The effects of Y-PPase mutations are also compared to the effects of the corresponding mutations in E-PPase on these same parameters, as measured by Salminen *et al.* (*12*), providing an interesting measure of the extent to which different portions of the active site are conserved between the two enzymes.

EXPERIMENTAL PROCEDURES

Enzymes. The expression and purification of the wild-type yeast PPase and its 14 active site variants from the overproducing *E. coli* HB101 strain transformed with suitable plasmids were carried out as described by Heikinheimo *et al.* (*18*). The proteins were stored at −70 °C with 20% glycerol. Glycerol was removed by dialysis prior to protein use.

Enzyme Assay. Initial rate measurements of PP_i hydrolysis were conducted by continuous recordings of P_i liberation obtained with an automatic P_i analyzer (*19*). Measurements were performed at constant $[Mg^{2+}]_{free}$ (20 mM) with varying concentrations of magnesium pyrophosphate as a substrate (*20*). Constant ionic strength ($\mu = 0.2$) was maintained by KCl in 0.1 M buffer (BIS-TRIS, TRIS, HEPES, CAPS) in the pH range 5.25−10.0, although variations in ionic strength between 0.12 and 0.2 had no significant effect on $k_{cat,app}$ or $K_{m,app}$ values. All rates were normalized against TRIS buffer and to a standard rate of wild-type PPase catalyzed reaction at pH 7.2. The total variation in the standard assay was ±20% for all samples tested. Reactions were carried out at 25 °C and were initiated by adding enzyme. Enzyme concentration was determined on the basis of a subunit molecular mass of 32 000 Da (*21*) and an $A^{1\%}_{280}$ equal to 14.5 (*22*).

Calculations. Values of equilibrium constants used to calculate the concentrations of $MgPP_i$ and Mg_2PP_i are presented in Table 1. Fitting of the kinetic equations used in this work (see below) was carried out by the program for nonlinear regression described by Duggleby (*23*). Values for $k_{cat,app}$ and $K_{m,app}$ were determined by computer fitting of apparent rate values as a function of total PP_i concentration to the Michaelis−Menten equation. Figures were drawn with the program ORIGIN from MicroCal software.

RESULTS

pH Profiles of WT-Y-PPase. $k_{cat,app}$ and $k_{cat,app}/K_{m,app}$ values for WT-Y-PPase catalysis of PP_i hydrolysis were determined over the pH range 5.25−9 at a fixed $[Mg^{2+}]_{free}$ of 20 mM. This concentration of Mg^{2+}, highly saturating for WT-Y-PPase, was chosen to minimize the effects that changes in Mg^{2+} affinity would have on changes in catalytic and equilibrium constants accompanying the mutations considered in this paper. Under these conditions, virtually all PP_i added is present as either $MgHPP_i$ or Mg_2PP_i, with the latter species becoming dominant above pH 6 (Table 1). For simplicity, we calculate $K_{m,app}$ values based on total PP_i concentration, since both 1:1 and 2:1 complexes of Mg^{2+} with PP_i are substrates for Y-PPase (*8, 10, 24*).

Both $k_{cat,app}$ and $k_{cat,app}/K_{m,app}$ display maxima as a function of pH (Figure 1). These profiles for the cloned enzyme are quantitatively similar to those reported by ourselves (*8, 25*) and others (*26*). The data were best fit to eqs 1a and 1b, which assume that $k_{cat,app}$ and $k_{cat,app}/K_{m,app}$ each depend on an essential base (with dissociation constants K_{ESH_2} and K_{EH_2}, respectively) and on an acid (with dissociation constants K_{ESH} and K_{EH}, respectively) and that, following ionization of the acid group, the enzyme retains some, albeit reduced, activity. From Table 2, k_{catH}, the first-order rate constant for ESH conversion to product, and k_{catH}/K_m, the second-order rate constant for EH reaction with S, are each 6−7 times larger than the corresponding rate constants, k_{cat} and k_{cat}/K_m, for the deprotonated species ES and E, respectively. This result is consistent with a recent detailed analysis of WT-Y-PPase activity as a function of both pH and $[Mg^{2+}]$ (G. A. Belogurov, A. A. Baykov, et al., manuscript in preparation).

$$k_{cat,app} = (k_{catH} + k_{cat}K_{ESH}/[H^+])/(1 + [H^+]/K_{ESH_2} + K_{ESH}/[H^+]) \quad (1a)$$

$$k_{cat,app}/K_{m,app} = (k_{catH}/K_m + (k_{cat}/K_m)K_{ESH}/[H^+])/(1 + [H^+]/K_{EH_2} + K_{EH}/[H^+]) \quad (1b)$$

where $K_m = [EH]_{ss}[S]/[EHS]_{ss}$ and the subscript ss refers to steady state.

pH Profiles of Y-PPase Variants. The pH−rate profiles of 12 out of 14 Y-PPase examined in this study are shifted to higher pH than WT-PPase, some markedly so. The two exceptions are the variants Y89F-PPase and E150D-PPase, which contain substitutions at positions that are no longer considered to be essential for activity (*18*). Thus, neither of these residues are directly involved in the binding of either P_i or Mn^{2+} in the EMn_4P_{i2} complex (*18*), and Glu 150 is not conserved evolutionarily, aligning with Gly 100 in *E. coli* PPase (*16*).

On the basis of the shapes of the pH profiles, the variants could be divided into three groups. Group I variants (Y89F, D115E, and E150D), like WT-PPase, have profiles for $k_{cat,app}$ and $k_{cat,app}/K_{m,app}$ clearly indicating appreciable (>5%) activity of the basic form versus the neutral form for the enzyme−substrate complex (ES and ESH, respectively) as well as for free enzyme (E and EH, respectively) (Figure 1). Group II variants have $k_{cat,app}$ and $k_{cat,app}/K_{m,app}$ profiles indicating little if any activity of the basic form of either enzyme−substrate complex or free enzyme. This group includes the variants E58D, R78K, and K193R. The largest of the three groups is group III and is characterized by a large, upward shift (>2.3 units) in pK_{ESH}, with the result that $k_{cat,app}$ reaches a plateau value at high pH (Figure 2). This group includes

Table 2: pH Profile Kinetic Parameters for PP_i Hydrolysis by Y-PPase

variant	group[a]	pK_{EH_2}	pK_{EH}	k_{catH}/K_m (10^6 M^{-1} s^{-1})	k_{cat}/K_m (10^6 M^{-1} s^{-1})	pK_{ESH_2}	pK_{ESH}	k_{catH} (s^{-1})	k_{cat} (s^{-1})	K_m (μM)
YWT		6.5 ± 0.1	7.9 ± 0.2	136 ± 14	15 ± 8	5.5 ± 0.1	7.7 ± 0.1	197 ± 9	29 ± 3	1.45
E48D	III	7.5 ± 0.1	8.8 ± 0.2	65 ± 6		7.1 ± 0.05	>10	78 ± 3		1.2
K56R	III	8.5 ± 0.2	9.2 ± 0.2	**0.17 ± 0.04**		8.5 ± 0.05	>10	16.9 ± 0.7		**99**
E58D	II	8.3 ± 0.2	9.4 ± 0.2	**1.4 ± 0.3**		8.3 ± 0.05	9.4 ± 0.1	17.8 ± 1.5		**13**
R78K	II	8.0 ± 0.2	9.0 ± 0.2	**4.1 ± 0.9**		7.4 ± 0.05	9.8 ± 0.05	111 ± 3		**27**
Y89F	I	6.8 ± 0.2	7.1 ± 0.2	197 ± 70	14 ± 11	6.0 ± 0.2	6.7 ± 0.2	130 ± 30	26 ± 1	0.7
Y93F	III	7.5 ± 0.1	8.8 ± 0.1	**3.7 ± 0.4**		7.2 ± 0.05	>10	15.5 ± 0.4		4
D115E	I	6.8 ± 0.1	7.8 ± 0.2	39 ± 7	2 ± 3	5.9 ± 0.05	7.9 ± 0.1	23 ± 1	2.4 ± 0.5	0.6
D117E	III	8.1 ± 0.1	9.2 ± 0.1	35 ± 8		8.9 ± 0.1	>10	28 ± 1		0.8
D120E	III	8.1 ± 0.2	8.7 ± 0.2	**0.61 ± 0.16**		9.2 ± 0.05	>10	**3.0 ± 0.1**		5
D147E	III	8.3 ± 0.1	≥9.5	**1.8 ± 0.2**		9.2 ± 0.1	>10	**7.4 ± 1.0**		4
E150D	I	6.3 ± 0.1	7.7 ± 0.1	70 ± 8	5.5	5.5 ± 0.1	7.4 ± 0.1	216 ± 20	47 ± 2	4
D152E	III	8.2 ± 0.1	9.2 ± 0.1	**0.11 ± 0.01**		8.1 ± 0.05	>10	**1.91 ± 0.05**		**17**
K154R	III	6.8 ± 0.1	8.3 ± 0.1	19.4 ± 1.8		6.6 ± 0.05	>10	51 ± 1		2.6
K193R	II	6.6 ± 0.1	8.9 ± 0.1	41.7 ± 2.5		6.5 ± 0.05	9.2 ± 0.1	57 ± 2		1.4

[a] Variants are divided into three different groups on the basis of their pH−rate profiles (see text). The most drastic effects on k_{cat}, k_{cat}/K_m, and K_m are shown in boldface.

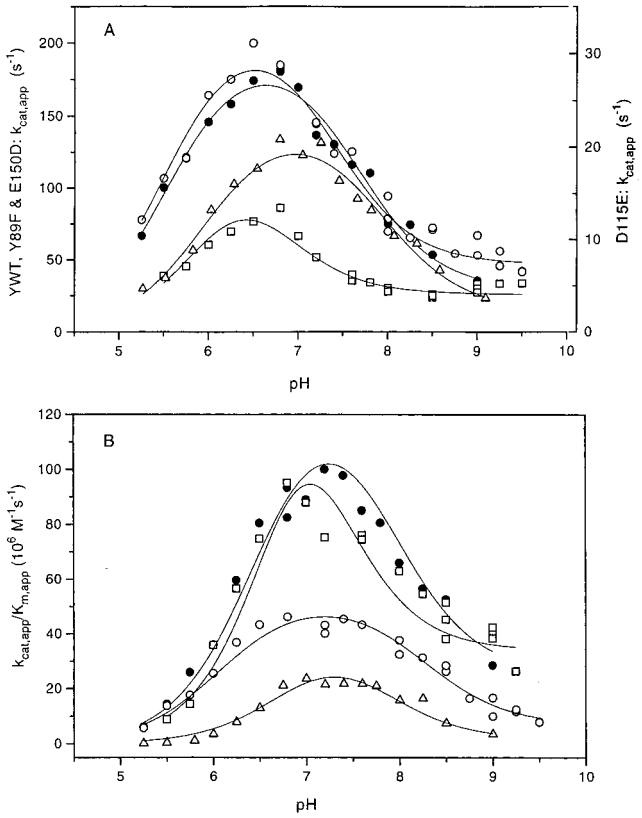

FIGURE 1: (A) Dependence of $k_{cat,app}$ on pH of WT-Y-PPase and group I Y-PPase variants. Lines are fit to eq 1a. Symbols: WT-Y-PPase (●), Y89F (□), D115E (△), and E150D (○). (B) Dependence of $k_{cat,app}/K_{m,app}$ of WT-Y-PPase and group I Y-PPase variants. Lines are fit to eq 1b. Symbols: WT-Y-PPase (●), Y89F (□), D115E (△), and E150D (○). Experimental conditions: 20 mM $[Mg]_{free}$ and $NaPP_i$ (1.5−1450 μM) in 0.1 M buffer (BIS-TRIS, TRIS, HEPES, CAPS) at the desired pH. Substrate concentrations were calculated as total PP_i (see text).

the remaining eight variants: E48D, K56R, Y93F, D117E, D120E, D147E, D152E, and K154R. The $k_{cat,app}/K_{m,app}$ profiles for these variants are similar to those for group II with the exception that $k_{cat,app}/K_{m,app}$ plateaus at high pH for D147E.

Values for the ionization constants, as well as for k_{catH}, k_{cat}, k_{catH}/K_m, k_{cat}/K_m, and K_m, determined by fitting the data to eqs 1a and 1b, are presented in Table 2.

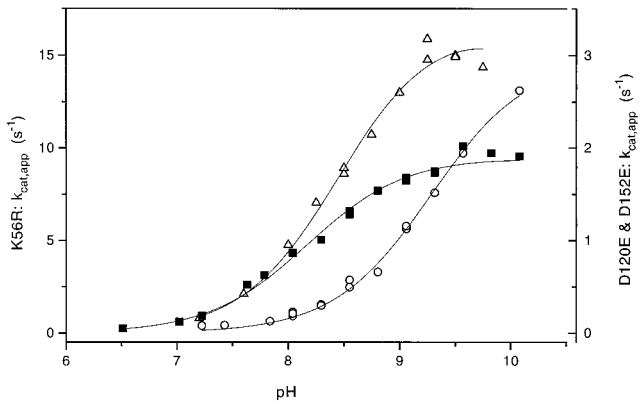

FIGURE 2: Dependence of $k_{cat,app}$ on pH for representative group III Y-PPase variants. Lines are fit to eq 1a. Symbols: K56R (△), D120E (○), and D152E (■). Conditions as in Figure 1.

DISCUSSION

Evidence for the fundamental functional and structural similarities of Y-PPase and E-PPase is quite overwhelming. As summarized in two recent articles (*5*, *14*), both enzymes require 3 to 4 divalent metal ions for maximal activity, each of the eight microscopic rate constants in the minimal kinetic scheme is closely similar between the two enzymes, some 14 to 15 polar active site residues are conserved [although overall sequence identity is only 27% (*14*)], and 154 (out of a total of 175) residues of Mg·E-PPase align with root mean square deviations of 1.40 and 1.45 Å from the Mn_2·Y-PPase and Mn_2·Y-PPase$(MnPi)_2$ structures, respectively (*5*). These structures provide an excellent framework for considering the effects on activity parameters of active site mutagenesis, as summarized in Table 2, as well as for comparing these effects with those measured earlier for the corresponding E-PPase variants (*12*), making the reasonable assumption that Mn(II) binding in sites M1−M4 parallels Mg^{2+} binding (*8*, *27*). The extent to which activity parameters change in the same or different ways in corresponding variants offers an interesting measure of how well portions of the active site are conserved. We use the term "corresponding variant" to refer to the same substitution made at aligned residues in Y-PPase versus E-PPase. For example, the corresponding variant E48/20D refers to E48D-Y-PPase and E20D-E-PPase.

Figure 3, reproduced from Heikinheimo *et al.* (*5*), recapitulates our current mechanistic proposal for PPase, as well

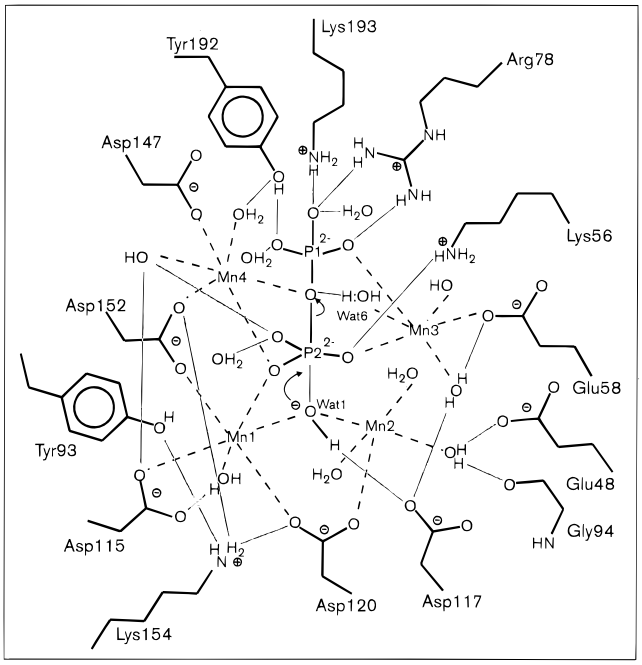

FIGURE 3: Mechanism and active site structure of Y-PPase as deduced from the crystal structure of the $Mn_2(MnP_i)_2$−Y-PPase complex [reprinted with permission from Heikinheimo *et al.* (*5*)]. Sites Mn1 and Mn2 are those occupied in the Mn_2E complex.

as many of the structural results at the active site, and is pertinent for the discussion of the results herein presented. In essence, we propose that PPase catalyzes PP_i hydrolysis by lowering the pK_a of the leaving group [Brønsted β 1.2 (*28*)], by forming an incipient hydroxide ion that functions as a stronger nucleophile than water, and by shielding the charge on the electrophilic phosphorus, thus permitting attack by the hydroxide anion. According to this mechanism, the leaving phosphoryl group is activated by coordination to R78, Y192, K193, M3, M4, and Wat6 (see below), the pK_a of the nucleophilic water is lowered by coordination to M1, M2, and perhaps D117 (see below), and the charge on the electrophilic phosphoryl group is neutralized through coordination to K56, Y93, and M1−M4.

Y-PPase vs E-PPase. Overall Comparison of pH Profiles. The pH profiles of $k_{cat,app}$ and $k_{cat,app}/K_{m,app}$ for wild-type Y-PPase and E-PPase are similar in that all four display pH optima but differ in that Y-PPase has lower pH optima and the base form of Y-PPase retains appreciable activity with respect to the neutral form [10−15% as measured by either k_{cat} or k_{cat}/K_m (Table 2)]. In contrast, the pH profiles of E-PPase are adequately fit assuming no activity for the basic form [i.e., k_{cat} in eqs 1a and 1b is set equal to zero (*11*−*13*)], although a level ≤5% for either parameter cannot be excluded.

The comparative effects of active site substitutions are summarized in Tables 3 (pH-independent parameters) and 4 (pK_as) and are analyzed in detail below. However, one generalization is immediately apparent. For almost every corresponding variant, the effects of substitution in raising the acid group pK_as, pK_{ESH} and pK_{EH}, are considerably greater in Y-PPase than in E-PPase. Since both pK_{ESH} (by 2 log units) and pK_{EH} (by 1.2 log units) are considerably lower in Y-PPase than in E-PPase, this result suggests that, on perturbation of the two active sites by mutation, the differences resulting in different pK_a values are relaxed; i.e., with respect to the acid group, corresponding variants are more similar than are the WT enzymes.

k_{catH} and K_m. With the exception of E150D, for which k_{catH} is slightly increased, all Y-PPase variants have decreased k_{catH} values compared to WT-Y-PPase. The largest effects are seen for three variants, D120E, D147E, and D152E, with relative values of 0.015, 0.04, and 0.010, respectively. Asp 120 binds to both metal ions M1 and M2 at the active site. The effect of D120E mutation parallels but is somewhat smaller than the very large effect seen for the corresponding D70E variant in E-PPase (Table 3), despite the fact that Mg^{2+} binding to this E-PPase variant in the absence of substrate is little affected (Hyytiä *et al.*, in preparation). We interpret these results as indicating that although Glu 120/70 binding to both M1 and M2 is retained in D120/70E, the distortion in the active site resulting from the need to accommodate an extra methylene group leads to a large decrease in catalytic activity, and this distortion is greater in E-PPase than in Y-PPase.

Asp 147 and Asp 152 fall within the Met 143−Trp 153 loop in Y-PPase that is one of two regions that differs the most between the Mn_2E and $Mn_2E(MnP_i)_2$ structures (*5*). This loop is drawn in more closely to the active site in the product complex, due in part to the binding of Asp 147 and Asp 152 to M4, with the result that the active site becomes less open to solvent and M1 and M2 are forced closer together. We suspect that the large effects seen on k_{catH} in the D147E and D152E variants reflect an interference with this structural change. The corresponding variants in E-PPase, D97E and D102E, have much smaller decreases in k_{catH} [relative values of 0.62 and 0.15, respectively (Table 3)], which is consistent with our finding that this region differs considerably between the E-PPase and Y-PPase structures [rmsd per Cα 1.94 Å (*5*)].

With respect to K_m, one variant, K56R, shows a very strong negative effect (60-fold rise) and three others, E58D, R78K, and D152E, show lesser, though still considerable, effects (10−20-fold rise). These results are in good accord with the active site structure depicted in Figure 3, since each of the four residues, Lys 56, Glu 58, Arg 78, and Asp 152, binds directly to one of the four product components (P1, P2, M3, and M4) and would also likely bind to substrate. However, two other variants containing substitutions for residues binding directly to substrate, K193R and D147E, show small or negligible effects on K_m. The corresponding six variants in E-PPase partition somewhat differently (Table 3). Two E-PPase variants, K29R and R43K, parallel the corresponding Y-PPase variants K56R and R78K in showing large increases in K_m, and the D97E variant parallels the Y-PPase D147E variant in having only a small effect on K_m, albeit in the opposite direction. However, the K142R variant in E-PPase also shows a large increase in K_m, whereas the change is small in the corresponding Y-PPase K193R variant, and the E31D and D102E variants in E-PPase show only minor effects on K_m, unlike the large changes in K_m seen in the corresponding Y-PPase E58D and D152E variants.

Essential Base pK_as. Again with the exception of the E150D variant, every Y-PPase substitution studied increased the pK_{ESH_2} by 0.4 to >3.7 log units (Table 2), with the largest changes resulting from the following substitutions: D120E, D147E > D117E > K56R > E58D > D152E. In an overall sense these results parallel very closely our earlier results

Table 3: pH-Independent Rate Parameters for *E. coli* and Yeast PPases[a]

		k_{catH}, rel		k_{catH}/K_m, rel		K_m (mM)	
yeast variant	*E. coli* variant	yeast	*E. coli*	yeast	*E. coli*	yeast	*E. coli*
WT	WT	1.00[c]	1.00[d]	1.00[e]	1.00[f]	1.45	4.3
E48D	E20D	0.40	0.65[g]	0.48	0.96[g]	1.2	2.9
K56R	K29R	0.09	0.07	0.0013	0.004	99	82
E58D	E31D	0.09	0.34	0.010	0.43	13	3.5
R78K	R43K	0.56	0.50	0.030	0.10	27	21
Y89F	Y51F	0.66	0.64[h,i]	1.4	nd[j]	0.7	nd[j]
Y93F	Y55F	0.08	0.24	0.027	(0.96)[k]	4	(0.96)[k]
D115E	D65E	0.12	0.46	0.29	0.93	0.6	2.1
D117E	D67E	0.14	0.23	0.26	1.07	0.8	0.9
D120E	D70E	0.015	<0.0005	0.004	<0.0002	5	
D147E	D97E	0.04	0.62	0.013	1.41	4	1.9
E150D	E101D	1.1	1.1[h,i]	0.51	nd[j]	4	nd[j]
D152E	D102E	0.010	0.15	0.0008	0.13	17	5.1
K154R	K104R	0.26	(1.15)[k]	0.14	(0.28)[k]	2.6	(18)[k]
K193R	K142R	0.31	1.42	0.31	0.07	1.4	83

[a] All values measured at 20 mM Mg^{2+}. [b] Relative activities of *E. coli* PPase variants are taken from Salminen *et al.* (*12*) except as otherwise indicated. [c] 197 s^{-1}. [d] 200 s^{-1}. [e] 0.46×10^8 M^{-1} s^{-1}. [f] 1.36×10^8 M^{-1} s^{-1}. [g] From Volk *et al.* (*29*). [h] From Käpylä *et al.* (*11*). [i] Measured at pH 8.0 only. [j] Not determined. [k] These values are less reliable (*12*).

Table 4: Essential Base and Acid ΔpK_as for *E. coli* and Yeast PPases[a]

		ΔpK_{EH_2}		ΔpK_{EH}		ΔpK_{ESH_2}		ΔpK_{ESH}	
yeast variant	*E. coli* variant	yeast	*E. coli*	yeast	*E. coli*	yeast	*E. coli*	yeast	*E. coli*
E48D	E20D	1.0	>0.8[b]	0.9	0.7[b]	1.6	1.1[b]	>2.3	0.5[b]
K56R	K29R	2.0	>2.5	1.3	0.7	3.0	2.9	>2.3	0.3
E58D	E31D	1.8	>1.9	1.5	0.1	2.8	1.7	1.7	0.7
R78K	R43K	1.5	>2.0	1.1	−0.2	1.9	1.6	2.1	−0.3
Y89F	Y51F	0.3	nd	−0.8	nd	0.5	nd	−1.0	nd
Y93F	Y55F	1.0	(>2.6)	0.9	(−0.5)	1.7	1.4	>2.3	−0.2
D115E	D65E	0.3	>2.9	−0.1	0.2	0.4	2.4	0.2	0.5
D117E	D67E	1.6	>2.0	1.3	0.1	3.4	2.4	>2.3	1.0
D120E	D70E	1.6	nd	0.8	(0)	3.7	nd	>2.3	(0)
D147E	D97E	1.8	>2.2	≥1.6	−0.5	3.7	1.5	>2.3	0.2
E150D	E101D	−0.2	nd	−0.2	nd	0.0	nd	−0.3	nd
D152E	D102E	1.7	>2.1	1.3	−0.3	2.6	1.7	>2.3	0.3
K154R	K104R	0.3	(>2.9)	0.4	(−0.2)	1.1	(2.75)	>2.3	(−0.3)
K193R	K142R	0.1	>2.0	1.0	0.1	1.0	2.1	1.5	−0.1

[a] All measured at 20 mM Mg^{2+}. *E. coli* data are from Salminen *et al.* (*12*), except as otherwise noted. Values in parentheses are less reliable. Values for WT enzyme are as follows: for yeast PPase, pK_{EH_2} 6.5 ± 0.1, pK_{EH} 7.9 ± 0.2, pK_{ESH_2} 5.5 ± 0.1, pK_{ESH} 7.7 ± 0.1; for *E. coli* PPase, pK_{EH_2} <6, pK_{EH} 9.1 ± 0.1, pK_{ESH_2} 6.6 ± 0.2, pK_{ESH} 9.7 ± 0.1. [b] From ref *29*.

with the corresponding E-PPase variants, which also show large increases in the value of pK_{ESH_2} compared with WT-E-PPase [Table 4 (*12*)]. The generality of these changes led us to propose (*12*) that the most likely candidate for an essential base in catalysis was an hydroxide ion, stabilized by binding to one or two metal ions at the active site, perhaps to an active site residue as well, and by an extended system of hydrogen bonds within the active site. This proposal was based on the expectation that any distortion of the active site that disrupts the interactions stabilizing the hydroxide ion would increase the pK_a of the bound water. Our present results, coupled with the recent structural results, showing a water/hydroxide ion (Wat1, the protonation state has not been determined) bridging metal ions M1 and M2 and hydrogen bonded to D117 (Figure 3), provide strong support for this proposal and suggest further that the hydroxide acts as a nucleophile in attacking the electrophilic phosphorus of enzyme-bound PP_i (*5*).

As with pK_{ESH_2}, virtually every Y-PPase substitution (the exceptions being E150D and K193R) increases pK_{EH_2} by 0.3−2.0 log units (Table 2), and the largest changes in pK_{EH_2} are observed for the same substitutions (K56R > E58D, D147E > D152E > D117E, D120E) giving the largest changes in pK_{ESH_2}. Although this result argues for a similarity in the nature of the groups having dissociation constants pK_{ESH_2} and pK_{EH_2}, they are presumably not identical, given the Y-PPase structural results (*5*) showing metal ions in sites M1 and M2 to be separated by two hydrogen-bonded waters in Mn_2E rather than the single water molecule seen in $Mn_2E(MnP_i)_2$ (Figure 3). We propose that pK_{EH_2} is the dissociation constant for loss of a proton from this two-water system. The most likely candidate is the water bound directly to M2, which retains the hydrogen bond to D117. Such an assignment is consistent with pK_{EH_2} being higher [1.0 log unit for WT-Y-PPase (Table 2)] than pK_{ESH_2}, since it would correspond to a water directly coordinated only to a single metal ion, and also provides a rationale for the observation that the effects of mutation on pK_{ESH_2} are somewhat larger than on pK_{EH_2} (Table 4).

Despite their overall similarities regarding the essential base, E-PPase does differ from Y-PPase in some respects. For example, in WT-E-PPase, pK_{EH_2} (<6) is lower than pK_{ESH_2} (6.6), and the effects of mutation on pK_{ESH_2} are more similar in magnitude to those on pK_{EH_2}. The latter may indicate no change in the nature of the ionizing group in EH_2 vs ESH_2, in contrast to what we have suggested for Y-PPase. Further differences are apparent in comparing substitution effects on pK_{ESH_2} and pK_{EH_2} for 11 corresponding variants in Y- vs E-PPase (Table 4). Particularly striking are the large effects E-PPase variants D65E, D104E, and

K142R show on both pK_{ESH_2} and pK_{EH_2} which are not seen with the corresponding Y-PPase variants D115E, D154E, and K193R. In addition, D147/97E, while showing similar effects on pK_{EH_2}, displays considerably larger effects on pK_{ESH_2} for Y-PPase than for E-PPase. This difference may be linked to differential movement of the 143−153 loop in Y-PPase versus the 93−103 loop in E-PPase following substrate binding, as mentioned above.

Acid pK_as. For 11 of the 14 variants studied in this paper, active site mutation raises the values of both pK_{ESH} (all but Y89F and E150D) and pK_{EH} (all but Y89F, D115E, and E150D), paralleling the results obtained with the essential base pK_a, as discussed above. For most variants, substitution effects are greater on pK_{ESH} than on pK_{EH}. Particularly dramatic are the $k_{cat,app}$ pH profiles for the the group III variants, for which the high pH descending limb is lost (Figure 2), indicating that the pK_as of the acid must be shifted to considerably higher pH than is true for WT-Y-PPase.

To what group in Y-PPase does pK_{ESH} correspond? We consider it likely that the activating acid protonates P1 during the hydrolysis reaction, thus activating it as a leaving group. The amino acid side chains that hydrogen bond to P1 [R78, K193, Y192 (Figure 3)] are unlikely candidates because variants of these residues in Y-PPase and of the aligned residues in E-PPase retain appreciable activity and do not show atypically large changes in the apparent pK_a of the general acid [Tables 2−4 (*12, 18*)]. We therefore believe the general acid is a water molecule hydrogen bonded to P1. A strong candidate is Wat6 in Figure 3 (*5*). The acidity of Wat6 would be expected to increase by coordination to M3, and, paralleling our earlier discussion of Wat1, the general rise in pK_a with mutation could reflect perturbation of the M3−Wat6 bond and of H-bonding interactions in which Wat 6 participates. It also is not unreasonable to speculate, based on the similarity of values of pK_{ESH} (7.9) and pK_{EH} (7.7) for WT-Y-PPase, that Wat6 is the modulating acid in EH as well, since deprotonation of this water could make substrate binding more difficult.

Catalytic and Dissociation Constants. There is an apparent correlation between the magnitude of the changes in the values of k_{catH} and of pK_{ESH_2} observed on active site substitution. The Y-PPase variants may be divided into two groups, those with $\Delta pK_{ESH_2} \leq 1.9$ log units and those with $\Delta pK_{ESH_2} \geq 2.6$ log units. Of the eight variants in the first group, six (E48D, R78K, Y89F, E150D, K154R, and K193R; the exceptions are Y93F and D115E) show relatively modest effects on k_{catH}, with values relative to k_{catH} for WT-Y-PPase of 0.26−1.1. In contrast, large effects on k_{catH} are observed for all six variants in the second group (K56R, E58D, D117E, D120E, D147E, and D152E), with values relative to k_{catH} for WT-Y-PPase of 0.01−0.14.

A similar correlation is evident between the values of k_{catH}/K_m and pK_{EH_2}. Here, six of the seven variants with $\Delta pK_{EH_2} \leq 1.0$ log unit (E48D, Y89F, D115E, E150D, K154R, and K193R; the exception is Y93F) have relative k_{catH}/K_m values of 0.14−1.4, whereas six of seven variants (K56R, E58D, R78K, D120E, D147E, and D152E; the exception is D117E)with ΔpK_{EH_2} 1.5−2.0 log units have relative k_{catH}/K_m values of 0.001−0.03.

The simplest interpretation of these correlations is that the changes in parameter values reflect, at least in part, substitution-induced distortions in active site structure and that, in general, larger distortions will give rise to larger changes in each of the parameters related to active site function.

Table 5: Comparing Mutation Effects in Corresponding Variants[a]

corresponding variant	k_{catH}	K_m	ΔpK_{ESH_2}	ΔpK_{EH_2}	class
E48/20D	S	S	S	S	S
K56/29R	S	S	S	S	S
E58/31D	S	S	S	S	S
R78/43K	S	S	S	S	S
Y93/55F	S	S	S	E	E
D115/65E	S	S	E	E	E
D117/67E	S	S	S	S	S
D120/70E	E	ND[b]	ND	ND	E
D147/97E	Y	S	Y	S	Y
D152/102E	Y	S	S	S	Y
K154/104R	S	E	E	E	E
K193/142R	S	E	S	E	E

[a] S indicates that the relative effects of mutation do not differ by more than a factor of 5 for the rate constants or by more than 1.2 log units for the dissociation constants, setting pK_{EH_2} for E-PPase equal to its upper limit of 6.0. Y and E indicate that mutation has a larger effect in Y-PPase or in E-PPase, respectively. [b] ND, not determined.

Y-PPases vs E-PPases. Similarities and Differences. Here we consider corresponding variant-induced changes in the four parameters k_{catH}, K_m, pK_{ESH_2}, and pK_{EH_2} as a measure of the similarity of portions of the active site of Y-PPase to the corresponding portions of the active site of E-PPase. The parameters pK_{ESH} and pK_{EH} are omitted in this consideration, since, as noted above, for almost every corresponding variant, the effects of substitution in raising pK_{ESH} and pK_{EH} are considerably greater in Y-PPase than in E-PPase, which would blur the distinctions we are seeking to explore.

As summarized in Table 5, the 12 corresponding variants break into three classes with respect to the four parameters under consideration: the S class, in which all four parameters show similar changes in both enzymes—E48/20D, E58/31D, K56/29R, R78/43K, and D117/67E; and the Y and E classes, in which one or more parameter changes are more marked either in Y-PPase—D147/97E and D152/102E—or in E-PPase—Y93/55F, D115/65E, D120/70E, K154/104R, and K193/142R, respectively. It is interesting that E48/20 is a member of the S class, despite the fact that the E20D-E-PPase variant has a somewhat destabilized quaternary structure (*29*), an effect not found in any of the Y-PPase variants herein considered (*18*). Also worth noting is that none of the variants is a hybrid, in the sense of having one parameter change more markedly in Y-PPase while another changes more markedly in E-PPase.

Importantly, each of the three classes, S, Y, and E, shows some spatial coherence. For example, four out of five residues in the E class, Y93/55, D115/65, D120/70 and K154/104, are also in close proximity (median and mean distances are 3.9 and 4.4 Å, respectively, as compared with values of 7.0 and 6.85 Å for Table 6 as a whole), forming much of the active site base (Figure 4). Of these, both the Y55F- and K104R-E-PPase variants have destabilized quaternary structures (*31*), which may account, at least in part, for the effects summarized in Table 5. These results support our view (*32*) that bacterial PPases represent close to a "minimal" PPase in which residues may be involved in more than one function, such that a substitution at the active site may affect the hydrophobic core and oligomeric stability as well. In addition, almost all of the intervening residues separating D65 in E-PPase from Y55 [Y55−S63 (*16*)], the nearest

Table 6: Distances between Side Chain Polar Termini[a]

	48S	56S	58S	78S	117S	147Y	152Y	93E	115E	120E	154E
56S	**5.25**										
58S	**3.98**	**2.73**									
78S	**9.78**	**4.57**	**4.26**								
117S	6.93	6.63	4.96	8.48							
147Y	12.44	7.58	8.39	6.56	8.54						
152Y	10.41	7.88	8.82	9.11	6.19	**3.32**					
93E	3.92	4.98	7.14	9.02	7.61	6.93	5.28				
115E	9.53	7.77	8.04	9.40	3.81	6.62	3.37	**6.77**			
120E	6.32	7.01	8.33	8.82	5.38	6.93	2.89	**3.03**	**4.80**		
154E	8.48	7.13	8.84	9.57	8.28	5.48	3.09	**2.86**	**6.02**	**2.62**	
193E	12.98	7.63	8.70	4.43	10.08	2.82	6.62	9.54	8.39	9.73	8.29

[a] Residues are grouped by class, S, Y, or E. Boldfaced distances demonstrate mutual proximity within the S, Y, and E groups.

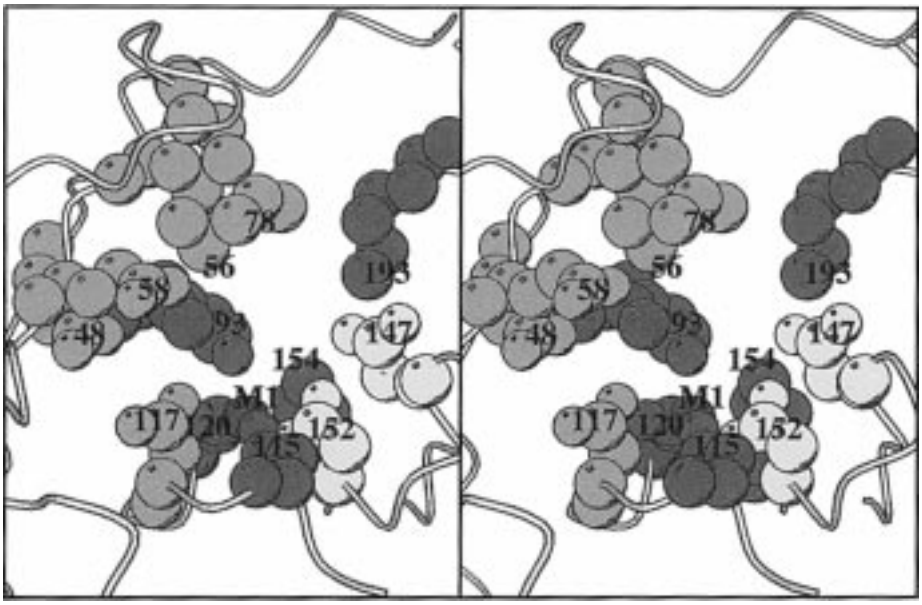

FIGURE 4: Active site structure in stereo emphasizing S (salmon), E (emerald green), and Y (yellow) regions. The path of the polypeptide backbone is shown as a gray ribbon, and the S, E, and Y amino acid side chains are shown at two-thirds van der Waals radius for clarity. As a result, the S wall formed by D48, K56, and E58 is in fact close-packed, unlike the appearance in the figure. The M1 manganese ion (also at two-thirds radius) is shown in maroon. The figure was produced using Molscript (*30*).

active site residue toward the N-terminus, are in a β-strand that is part of the core PPase structure. The relative rigidity of this connection would be expected to result in a stronger sensitivity of the catalytic center toward substitution at these residues than is the case for substitution at the corresponding positions in Y-PPase, i.e., D115 and Y93, which are connected by 18 additional residues that form a flexible loop (Figure 3 in ref *5*).

The two residues in the Y class, D147/97, and D152/102, are also in close proximity (3.3 Å), and as described above, the greater sensitivity of Y-PPase catalytic parameters to mutation at these positions may be linked to differential mobility of the 143−153 loop in Y-PPase versus the 93−103 loop in E-PPase. The Y and E class residues provide a clear demonstration that, even in the context of a highly conserved active site, corresponding mutations can have different effects on catalytic function, presumably because of interactions of the mutated site with portions of the enzymes outside the active site, which are less well conserved.

Finally, and perhaps of greatest interest, four of five residues in the S class, E48/20, K56/29, E58/31, and R78/43 are in close proximity (the median and mean distances among these residues are 4.4 and 5.1 Å, respectively), forming one wall of the active site cavity, and the fifth residue, D117/67, though somewhat farther away, is on the same side of the cavity (Figure 4). As corresponding mutations in the portion of the active site defined by these residues have essentially the same functional effects, this portion of the active site can be considered to be the most highly conserved evolutionarily.

What is the significance of such conservation? One possible response, which we are currently investigating, is that groupings of acid and base residues with spacings and orientations similar to those in the S class are a common feature of phosphoryl-transfer enzymes. A second, much more speculative and difficult to test, is that these residues might be the vestige of the active site of a primitive ur-PPase. Here, referring to Figure 3, we note that the necessary functions of a PPase are included in the S class residues. Thus: (a) activation of the leaving phosphoryl group in P1 could be provided by interaction with R78 and M3, the latter bound through interaction with E58; (b) charge shielding of the electrophilic group in P1 could be provided by interaction with K56 and M2, the latter bound via a water molecule held in place by E48; and (c) activation of the nucleophilic

water could be provided by D117 acting as a general base and coordination to M2. According to this speculation, optimization of the active site through the addition of further Lewis acid residues (K154, K193, Y93, Y192) and metal ions (M1, M4) came later. That a more minimalist PPase may still exist is suggested by the detection of PPase activity in *Methanococcus jannaschii* (*33*), despite the failure of standard sequence comparisons to locate a PPase in the genome sequence of this archaeabacterium (*34*). Indeed, Baltscheffsky *et al.* (*35*) have identified a hypothetical protein within the *M. jannaschii* genome (MJ0882) that aligns so as to conserve several of the 14 to 15 conserved PPase active site residues, including 4 from within the S class: identical matches at K56/29 and D117/67, with an Asp in place of E48/20 and a Lys in place of R78/43 (H. Baltscheffsky, personal communication).

Extrapolating from Table 5 and our structural studies (*5*), we may predict that the large degree of active site residue overlap found on comparing the structures of WT-Y-PPase and WT-E-PPase (an rmsd of 0.4 Å per Cα) will be largely conserved in the S-class variants. On the other hand, the rmsd should increase for the E-class variants, due to the pleiotropic nature of substitutions at the base of the E-PPase active site, but possibly not for the Y-class variants, because these residues (D147/97 and D152/102) fall in a loop that is both flexible and already very different between the two wild-type PPases. As structural studies of the variants are currently underway, both in our laboratories and in the laboratories of Harutyunyan and Avaeva (*36*, *37*), a test of these predictions should be forthcoming.

ACKNOWLEDGMENT

We thank Vesa Tuominen for help with calculations and with Figure 4, Dante Still for computing support, and Alex Baykov for helpful discussions.

REFERENCES

1. Chen, J., Brevet, A., Fromant, M., Leveque, F., Schmitter, J.-M., Blanquet, S., and Plateau, P. (1990) *J. Bacteriol. 172*, 5686−5689.
2. Lundin, M., Baltscheffsky, H., and Ronne, H. (1991) *J. Biol. Chem. 266*, 12168−12172.
3. Sonnewald, U. (1992) *Plant J. 2*, 571−581.
4. Kornberg, A. (1962) in *Horizons in Biochemistry* (Kasha, M., and Pullman, B., Eds.) p 251, Academic Press, New York.
5. Heikinheimo, P., Lehtonen, J., Baykov, A. A., Lahti, R., Cooperman, B. S., and Goldman, A. (1996) *Structure 4*, 1491−1508.
6. Springs, B., Welsh, K. M., and Cooperman, B. S. (1981) *Biochemistry 20*, 6384−6391.
7. Cooperman, B. S. (1982) *Methods Enzymol. 87*, 526−548.
8. Welsh, K. M., Jacobyansky, A., Springs, B., and Cooperman, B. S. (1983) *Biochemistry 22*, 2243−2248.
9. Gonzalez, M. A., Webb, M. R., Welsh, K. M., and Cooperman, B. S. (1984) *Biochemistry 23*, 797−801.
10. Baykov, A. A., and Shestakov A. S. (1992) *Eur. J. Biochem. 206*, 463−470.
11. Käpylä, J., Hyytiä, T., Lahti, R., Goldman, A., Baykov, A. A., and Cooperman, B. S. (1995) *Biochemistry 34*, 792−800.
12. Salminen, T., Käpylä, J., Heikinheimo, P., Kankare, J., Goldman, A., Heinonen, J., Baykov, A. A., Cooperman, B. S., and Lahti, R. (1995) *Biochemistry 34*, 782−791.
13. Baykov, A. A., Hyytiä, T., Volk, S. E., Kasho, V. N., Vener, A. V., Goldman, A., Lahti, R., and Cooperman, B. S. (1996) *Biochemistry 35*, 4655−4661.
14. Cooperman, B. S., Baykov, A. A., and Lahti, R. (1992) *Trends Biochem. Sci. 17*, 262−266.
15. Baykov, A. A., and Avaeva, S. M. (1973) *Eur. J. Biochem. 32*, 136−142.
16. Kankare, J., Neal, G. S., Salminen, T., Glumoff, T., Cooperman, B. S., Lahti, R., and Goldman, A. (1994) *Protein Eng. 7*, 823−830.
17. Terzyan, S. S., Voronova, A. A., Smirnova, E. A., Kuranova, I. P., Nekrasov, Y. V., Arytyunyan, E. G., Vainshtein, B. K., Höhne, W. E., and Hansen, G. (1984) *Bioorg. Khim. 10*, 1469−1482.
18. Heikinheimo, P., Pohjanjoki, P., Helminen, A., Tasanen, M., Cooperman, B. S., Goldman, A., Baykov, A. A., and Lahti R. (1996) *Eur. J. Biochem. 239*, 138−143.
19. Baykov, A. A., and Avaeva, S. M. (1981) *Anal. Biochem. 116*, 1−4.
20. Volk, S. E., Baykov, A. A., Duzhenko, V. S., and Avaeva, S. M. (1982) *Eur. J. Biochem. 125*, 215−220.
21. Kolakowski, L. F., Jr., Schloesser, M., and Cooperman, B. S. (1988) *Nucleic Acids Res. 16*, 10441−10452.
22. Kunitz, M. (1952) *J. Gen. Physiol. 35*, 423−450.
23. Duggleby, R. (1984) *Comput. Biol. Med. 14*, 447−455.
24. Moe, O. A., and Butler, L. G. (1972) *J. Biol. Chem. 247*, 7308−7314.
25. Konsowitz, L. M., and Cooperman, B. S. (1976) *J. Am. Chem. Soc. 98*, 1993−1995.
26. Knight, W. B., Fitts, S. W., and Dunaway-Mariano, D. (1981) *Biochemistry 20*, 4079−4086.
27. Cooperman, B. S., Panackal, A., Springs, B., and Hamm, D. J. (1981) *Biochemistry 20*, 6051−6060.
28. Benkovic, S. J., and Schray, K. J. (1973) in *The Enzymes, 3rd Ed*. (Boyer, P. D., Ed.) Vol. 8, pp 201−238, Academic Press, New York.
29. Volk, S. E., Dudarenkov, V. Y., Käpylä, J., Kasho, V. N., Voloshina, O. A., Salminen, T., Goldman, A., Lahti, R., Baykov, A. A., and Cooperman, B. S. (1996) *Biochemistry 35*, 4662−4669.
30. Kraulis, P. J. (1991) *J. Appl. Crystallogr. 24*, 945−950.
31. Fabrichniy, I. P., Kasho, V. N., Hyytiä, T., Salminen, T., Halonen, P., Dudarenkov, V. Yu., Heikinheimo, P., Chernyak, V. Ya., Goldman, A., Lahti, R., Cooperman, B. S., and Baykov, A. A. (1997) *Biochemistry 36*, 7746−7753.
32. Kankare, J., Salminen, T., Lahti, R., Cooperman, B. S., Baykov, A. A., and Goldman, A. (1996) *Acta Crystallogr. D52*, 551−563.
33. Schäfer, T., and Schäfer, G. (1997) in *Proceedings of the 1st International Meeting on Inorganic Pyrophosphatases* (Lahti, R., Ed.) Turku, Finland, pp 9−12, University of Turku, Turku, Finland.
34. Bult, C. J., White, O., Olsen, G. J., Zhou, L., Fleischmann, R. D., Sutton, G. G., Blake, J. A., FitzGerald, L. M., Clayton, R. A., Gocayne, J. D., Kerlavage, A. R., Dougherty, B. A., Tomb, J. F., Adams, M. D., Reich, C. I., Overbeek, R., Kirkness, E. F., Weinstock, K. G., Merrick, J. M., Glodek, A., Scott, J. L., Geoghagen, N. S. M, Weidman, J. F., Fuhrmann, J. L., and Venter, J. C. (1996) *Science 273*, 1058−1073.
35. Baltscheffsky, H., Baltscheffsky, M., Nadanaciva, S., Persson, B., and Schultz, A. (1997) in *Proceedings of the 1st International Meeting on Inorganic Pyrophosphatases* (Lahti, R., Ed.) Turku, Finland, pp 1−3, University of Turku, Turku, Finland.
36. Harutyunyan, E. H., Kuranova, I. P., Vainshtein, B. K., Höhne, W. E., Lamzin, V. S., Dauter, Z., Teplyakov, A. V., and Wilson, K. S. (1996a) *Eur. J. Biochem. 239*, 220−228.
37. Harutyunyan, E. H., Oganessyan, V. Yu., Oganessyan, N. N., Terzyan, S. S., Popov, A. N., Rubinsky, S. V., Vainshtein, B. K., Nazarova, T. I., Kurilova, S. A., Vorobyeva, N. N., and Avaeva, S. M. (1996b) *Kristallografia 41*, 84−96.

BI971771R